Physica B 460 (2015) 214–217

Contents lists available at ScienceDirect

Physica B

journal homepage: www.elsevier.com/locate/physb

Thermodynamic and neutron diffraction studies on multiferroic $NdMn_2O_5$

S. Chattopadhyay [a], V. Balédent [a], P. Auban-Senzier [a], C. Pasquier [a], C. Doubrovsky [a], M. Greenblatt [b], P. Foury-Leylekian [a,*]

[a] Laboratoire de Physique des Solides, Université Paris-Sud, CNRS-UMR 8502, 91405 Orsay, France
[b] Department of Chemistry and Chemical Biology, Rutgers, The State University of New Jersey, Piscataway, NJ 08854, USA

ARTICLE INFO

Available online 24 November 2014

PACS:
75.25.−j
77.22.Ch
75.30.Et
61.05.cp
61.05.F−

Keywords:
Multiferroic
Magnetic susceptibility
Dielectric permittivity
Neutron diffraction

ABSTRACT

Magnetically frustrated RMn_2O_5 oxides have attracted considerable attention in recent years, because most of the members of this family show spin ordering induced dielectric polarization along with strong magneto-electric coupling. Although the true origin of the ferroelectricity is still a matter of debate, it has been observed that the magneto-electric phase diagram can be substantially tuned with the variation of rare earth elements. In this work, we have chosen $NdMn_2O_5$ as the compound of our interest since it lies exactly in between the ferroelectric and non-ferroelectric members of this family and also, because there are few investigations performed on RMn_2O_5 systems with large rare earth atoms . With the combination of heat capacity, magnetic susceptibility, dielectric permittivity, powder X-ray diffraction, and powder neutron diffraction measurements, it has been found that $NdMn_2O_5$ undergoes an incommensurate magnetic ordering around 30 K followed by a possible ferroelectric-like transition at ~26 K. Another lock-in kind of magnetic transition appears when the temperature is decreased to ~15 K. With further lowering of temperature, an antiferromagnetic ordering, which is presumably associated with the Nd^{3+}, is achieved near 4 K. This study thus sheds light on a new compound of the RMn_2O_5 series presenting different multiferroic properties.

1. Introduction

In recent years, a special kind of multiferroic materials popularly known as *magnetic ferroelectrics* has attracted considerable attention because of their potentiality for both fundamental and technological aspects [1,2]. The reason behind such significant interest lies in the exotic and complex nature of their magnetic and electric phase diagrams. To be more specific, it has been found that the ferroelectricity, which appears in this family of compounds at low temperature (T), is associated with the magnetic ordering signifying the presence of an important coupling between the spin and charge degrees of freedom.

In this category of multiferroics, geometrically frustrated RMn_2O_5 (R=Y and lanthanide) type oxides are of special interest mainly due to the strong magneto-electric coupling observed in this series [1,3,4]. The room temperature crystal structure of RMn_2O_5 is centrosymmetric with orthorhombic space group *Pbam* [5,6]. The Mn ions are present in two valence states and form $Mn^{3+}O_5$ and $Mn^{4+}O_6$ type square pyramidal and octahedral environments (Fig. 1), respectively, with the surrounding oxygen ions. Mn^{4+} ions form chain-like arrangement along the crystallographic c direction in the presence of two dominant super-exchange interactions $J1$ and $J2$ along c. In addition, zig-zag chains of Mn ions run along the a direction. In the a,b plane loops of Mn ions are formed. Each loop is composed of five Mn ions (three Mn^{3+} and two Mn^{4+}) which are magnetically coupled to each other by three types of nearest neighbor interactions $J3$, $J4$, and $J5$ [7,8]. Since all of them are antiferromagnetic in nature, this leads to magnetic frustration in this series.

RMn_2O_5 with small R^{3+} ions are well-known to show multiple magnetic transitions [9,10]. In general, an incommensurate magnetic (ICM1) state appears near 40 K followed by a commensurate magnetic (CM) one at slightly lower temperature. With further cooling, another ICM state (ICM2) evokes and finally, R^{3+} ions magnetically order generally below 10 K. Moreover, the ferroelectricity (FE) is always seen to appear concurrently with the CM state. It is proposed that in the CM phase, Mn^{3+} ions shift due to the exchange striction effect and break the inversion symmetry paving the way for FE [1]. However, the actual microscopic origin of the spin-induced ferroelectricity in these compounds is still a matter of great debate due to the difficulty to detect the Mn displacement and due to the very complex and diverse magnetic

* Corresponding author. Fax: +33 169156086
E-mail address: pascale.foury@u-psud.fr (P. Foury-Leylekian).

http://dx.doi.org/10.1016/j.physb.2014.11.074
0921-4526/

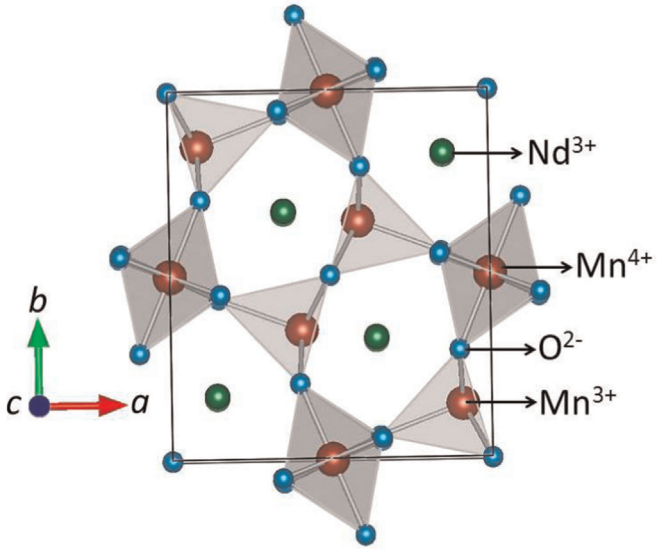

Fig. 1. A perspective view of the crystal structure of $NdMn_2O_5$ in the *a,b* plane. Here, Nd^{3+}, Mn^{3+}, and Mn^{4+} ions are all magnetic entities, while it is only Mn^{3+}, which is believed to be related to the onset of ferroelectricity.

phases. Particularly, understanding the role of the rare earth ions on the magnetic ordering and ferroelectricity is lacking. It is to be noted that the phase transitions can be tuned significantly by the nature of the rare earth ion. For example, RMn_2O_5 oxides with large R^{3+} ions (La, Pr) do not show FE in contrast to their counterparts with smaller rare earth ions (Sm to Lu) [6,8,9,11]. Unfortunately, most of the investigations performed on RMn_2O_5 oxides deal with the compositions with R^{3+} ions with small ionic radii. Although, studies on the members with large rare earth ions can play a crucial role to shed light on the ambiguous issues, there are few investigations on these compositions [8,11–13] due to difficulty in synthesis.

Keeping these facts in mind we have chosen to investigate $NdMn_2O_5$. In addition, this compound has a speciality as it lies exactly in between the ferroelectric Sm and non-ferroelectric Pr based members of this family. Detailed thermodynamic, dielectric, X-ray and neutron diffraction studies have been performed to gain more insight about the compositional variation of the magnetic order and the ferroelectric character in RMn_2O_5 family as far as the rare earth ion is concerned.

2. Sample preparation and experimental details

Polycrystalline sample of $NdMn_2O_5$ was synthesized following the method as described in reference [14] using highly pure Nd_2O_3 and metallic Mn in stoichiometric ratio. Nd_2O_3 was initially heated for 24 h at 650 °C for drying, while metallic Mn was initially washed with dilute HCl and acetone. Both the ingredients were dissolved in HNO_3 solution and dried overnight at 250 °C. The obtained precursor was again heated at 600 °C for 12 h in alumina crucible. After this heat treatment, the powder was ground thoroughly and pressed into pellets. The final sintering was performed with these pellets at 1100 °C for 48 h under oxygen flow.

Heat capacity (C_p) measurement was performed in a Physical Property Measurement System (PPMS). Magnetization (M) measurement was carried out using a SQUID magnetometer. Dielectric permittivity (ϵ) was measured with an RLC bridge instrument. High resolution powder X-ray diffraction experiment was conducted at the CRISTAL beam-line of Soleil synchrotron source in France. Powder neutron diffraction studies were performed in G4.1 diffractometer from Orphée-LLB facility in France.

3. Results

3.1. Heat capacity

Fig. 2 depicts the variation of C_p/T as a function of temperature for $NdMn_2O_5$ between 3 K and 50 K. One can easily notice the presence of multiple anomalies in the plot. Starting from high-T side, the first anomaly appears near $T=30$ K (T_1) as a broad peak. It is followed by another weak anomaly near 26 K (T_2). With further cooling, a shoulder like feature appears around 17 K (T_3), and finally a very sharp peak can be observed near 4 K (T_4). We have checked reliability of all the features observed by repeating the measurement.

3.2. Magnetic susceptibility

To probe whether the transitions observed in C_p have magnetic origin, we performed dc magnetization measurement. Fig. 3 shows temperature variation of dc magnetic susceptibility χ (M/H, H being the applied magnetic field) between 2 K and 140 K measured in zero field cooled (ZFC) and field cooled (FC) protocols under $H=100$ Oe. The ZFC curve shows a distinct hump like feature around $T' = 36$ K i.e. close to T_1, followed by another weak anomaly around T_3 (~15 K). Moreover, a broad peak can be observed exactly at T_4 (~4 K) in agreement with the C_p data. However, no anomaly is present near T_2. The FC data also carries signature of all these transitions as observed in the ZFC curve. Interestingly, ZFC and FC curves show thermomagnetic irreversibility below 120 K. Such bifurcation is usually found in superparamagnetic and spin glass like systems due to blocking of noninteracting moments or cooperative freezing of spins. However, by performing ac susceptibility measurement, we have discarded these two possibilities since there is no shift of the peak with varied frequency. Thus, for the present system, the ZFC-FC bifurcation seems to be related to the spin fluctuation due to geometrical frustration. The high-T part of the ZFC and FC curves follow typical Curie–Weiss type paramagnetic behavior as $\chi = C/(T-\theta)$, where C and θ denote the Curie constant and the Curie–Weiss temperature, respectively. By fitting the ZFC curve with this equation, we obtained $\theta = -161$ K signifying strong antiferromagnetic correlations, and $C=3.78$ emu K/mol. Also, the

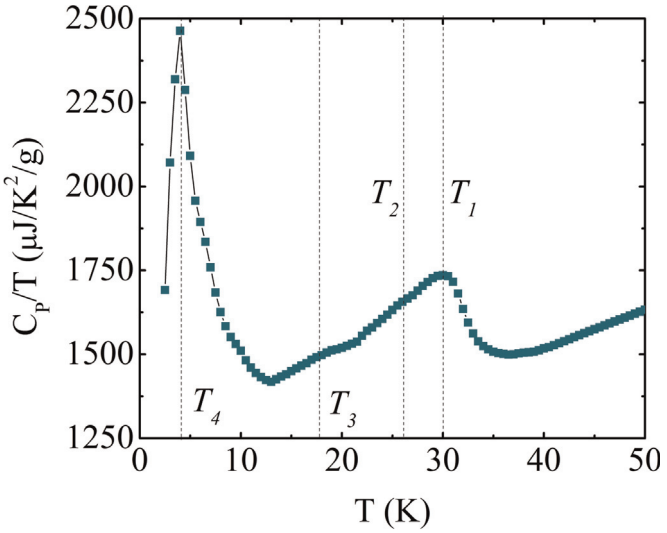

Fig. 2. Temperature (T) variation of heat capacity (C_P) over T for $NdMn_2O_5$ sample.

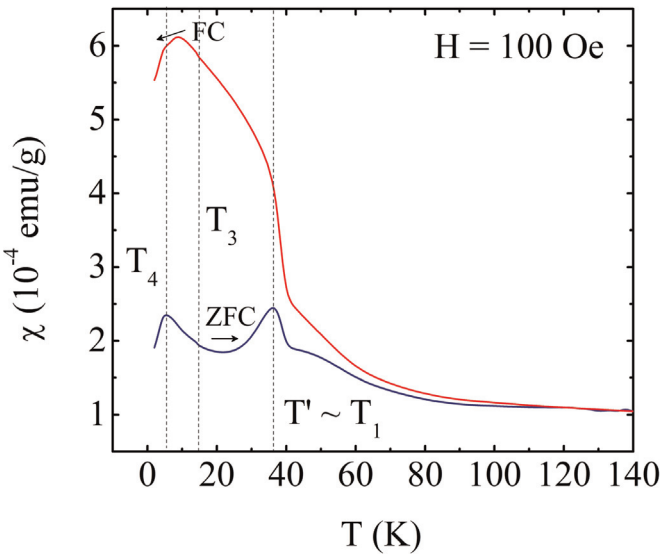

Fig. 3. T dependence of dc magnetic susceptibility (χ) measured in zero field cooled (ZFC) and field cooled (FC) protocols.

mean effective moment per formula unit was calculated to be 3.2 μ_B. It is well known that the ratio $|\theta/T'|$ reflects the strength of frustration. For our case it is ~4.5 implying that $NdMn_2O_5$ is moderately frustrated [15]. It also provides support to our hypothesis that the thermomagnetic irreversibility is related to the frustration.

3.3. Dielectric permittivity

In RMn_2O_5 family, study of the dielectric properties has always been an important aspect as it is closely connected to the multiferroicity. For $NdMn_2O_5$, we performed dielectric permittivity measurement as a function of T. Fig. 4 displays temperature variation of the real part of dielectric permittivity (ϵ') with varied frequency (f=1, 10, and 100 kHz). With decreasing temperature, ϵ' shows a sharp peak at ~25 K i.e. around T_2. The peak position does not vary with f excluding the possibility of any thermally activated or relaxor like behavior and emphasizing the onset of a ferroelectric-like transition around T_2. It is to be mentioned that the multiferroic members of RMn_2O_5 (such as $GdMn_2O_5$ and $TbMn_2O_5$) family show a very similar feature like this around ICM1

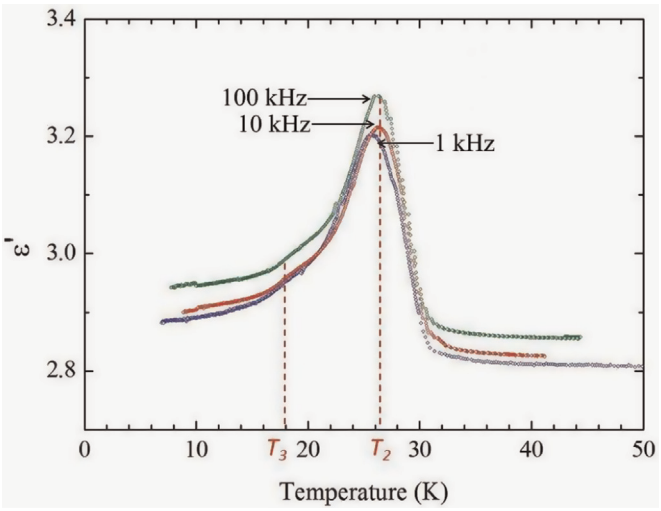

Fig. 4. Real part of dielectric permittivity (ϵ') as a function of T with varied frequency.

to CM transition signifying emergence of the ferroelectric state. A careful look at the $\epsilon'(T)$ unveils another weak anomaly near 18 K (~ T_3). For some other RMn_2O_5 multiferroics (for example in $TbMn_2O_5$), this feature has been found to be connected with *electromagnon* excitation related to magneto-electrically coupled systems [16,17]. For $NdMn_2O_5$, further investigation can be performed to characterize this feature.

3.4. X-ray diffraction

High resolution X-ray diffraction (XRD) measurement on powder was performed at 300 K and 3 K using synchrotron source to study the crystallographic parameters and the possible structural modifications associated with the ferroelectric-like transition. It is evident from the Rietveld refinement at room temperature that $NdMn_2O_5$ can be indexed according to *Pbam* space group as expected. The system retains this structure down to 3 K, while in the ferroelectric phase, we expect the loss of the *a* glide mirror of the *Pbam* space group. Indeed, this leads to the loss of the center of inversion, a mandatory condition for ferroelectricity. The loss of the *a* glide mirror would be characterized by the appearance of weak Bragg reflections at *h0l* with *h* odd, forbidden in the *Pbam* space group. None of these reflections have been observed in the powder X-ray diffractogram. In addition, in case of a strong exchange striction effect, the appearance of satellite reflections at 2*q* (where *q* is the magnetic propagation vector) is expected. No such reflections have been detected. However, the sensitivity of powder diffraction to such weak structural effects is probably not sufficient and single crystal measurements are certainly necessary to investigate further the structural impacts of the magnetic and ferroelectric phases.

3.5. Neutron diffraction

Powder neutron diffraction (PND) measurements on $NdMn_2O_5$ were carried out between 2 K and 300 K. Firstly, we wanted to have precise oxygen positions and their temperature evolution particularly around T_2, since it could provide some hints about the possible symmetry breaking around the ferroelectric-like transition at T_2. Secondly, we also wished to have microscopic characterization of the magnetic transitions observed in the bulk thermodynamic measurements. However, careful analysis based on Rietveld method reveals that there is no significant displacement of the Mn^{3+} ions and O^{2-} ions forming MnO_5 square pyramids between 300 K and 2 K. This result strengthens our inference from XRD analysis that the structural effect associated with the ferroelectric-like transition is certainly too weak to be detected in powder measurements, which is also in line with the observation made by Koo et al. in $TbMn_2O_5$ [10].

However, from the PND profiles measured at different T, it can be observed that a new set of reflections appears below 30 K (Fig. 5). These newly generated reflections can readily be ascribed as magnetic satellites since no additional reflections were observed in XRD in this temperature range. Moreover, these magnetic satellites shift to higher diffraction angle with decreasing T, reflecting ICM character of the magnetic propagation vector q. An attentive look reveals the presence of splitting in some of the magnetic reflections. These split reflections cannot be fitted with one propagation vector. We tentatively tried to fit the PND profiles below 30 K using FullProf software [18] and found that there are actually two ICM propagation vectors q_1=(0.5, 0, 0.4-δ) and q_2=(0.5, 0, 0.398) between 28 K and 15 K. Fig. 6 depicts T variation of the c^* component of the propagation vector (q_l) extracted from the fitting. As can be seen, q_{l1} increases with decreasing temperature below T_1 and merges with q_{l2} at 15 K which is close to T_3. A lock-in kind of transition sets in at this temperature, below

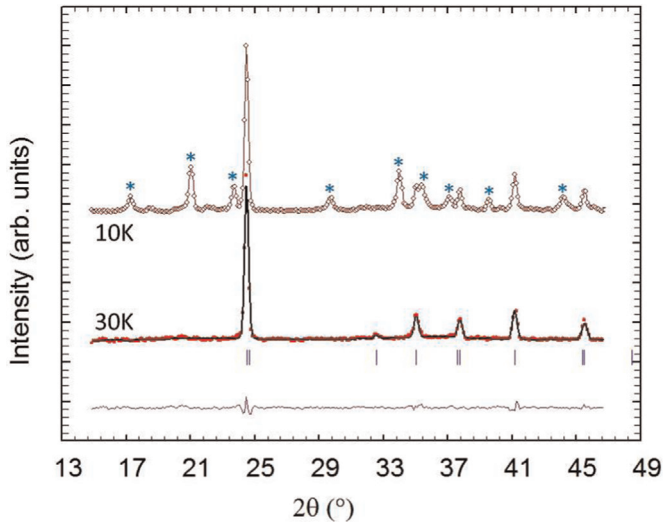

Fig. 5. Powder neutron diffraction data recorded at 30 K (with Rietveld refinement) and 10 K. For 10 K data, '*' symbol denotes the magnetic satellites.

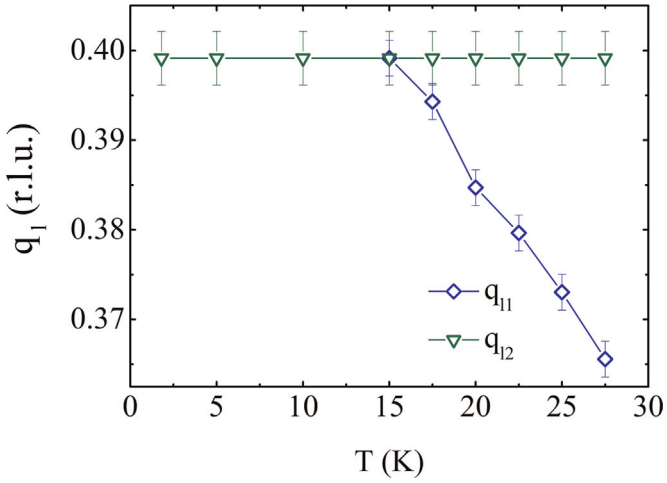

Fig. 6. Temperature evolution of the c^* components of the magnetic propagation vector q_{li}.

which no evolution of q_{l2} is observed. It is important to mention that the nature of the temperature evolution of the magnetic propagation vectors is to some extent different than the result obtained by Zobkalo et al. recently [13]. Our PND data also shows that finally below 5 K ($\sim T_4$), another propagation vector q_3=(0.5, 0, 0) emerges (not shown) which coexists with q_2. In general at low temperature, R^{3+} moments order following the same propagation vector as the Mn moments. In case of $NdMn_2O_5$, the observation of the q_3 propagation wave vector below 5 K seems to indicate that the R^{3+} spins order differently than the Mn spins. This is also seen in $DyMn_2O_5$ [9].

4. Conclusion

In conclusion, we synthesized polycrystalline sample of $NdMn_2O_5$ and performed detailed thermodynamic, dielectric, X-ray, and neutron diffraction measurements. Analyses based on the results unveil that this composition undergoes multiple phase transitions at low temperature. Around $T_1 \sim 30$ K, a ICM phase appears with two incommensurate magnetic propagation vectors with slightly different c^* components. With decreasing temperature, a ferroelectric-like state presumably emerges at $T_2 \sim 26$ K followed by a lock-in type transition around $T_3 \sim 15 \pm 2$ K. Finally at $T_4 \sim 4$ K, another magnetic transition is observed which is possibly associated with the ordering of Nd^{3+} moments. Although the phase transitions observed in $NdMn_2O_5$ are somewhat similar to the transitions in other RMn_2O_5 compositions with small R^{3+} ions, it is the characteristic of the possible ferroelectric-like state that discriminates $NdMn_2O_5$ from the other members of this family and makes it unique. Interestingly, here the ferroelectric-like state appears in the ICM phase in contrast to the other RMn_2O_5 oxides, where FE always appears concurrently with the CM state. With such a distinctive feature, this composition really demands further investigation particularly focusing on the behavior of the electric polarization and the magnetic structure in the ferroelectric state. Such investigation is already in progress and hopefully, it will be able to provide deeper understanding on the origin of FE and the role of rare earth ions on it.

Acknowledgments

We acknowledge SOLEIL for the provision of synchrotron radiation beam time and we would like to thank E. Elkaim for his assistance in using CRISTAL beam-line. We also acknowledge LLB for the provision of neutron beam time and we thank G. André for the help in using beam-line G4.1. We are also thankful to F. Damay for her help regarding PND data analysis. This work is supported by a public grant from the Laboratoire d'Excellence Physics Atom Light Mater (LabEx PALM) overseen by the French National Research Agency (ANR) as part of the Investissements d'Avenir program (reference: ANR-10-LABX-0039). The work by M.G. was supported by NSF-DMR - 0966829.

References

[1] S.W. Cheong, M. Mostovoy, Nat. Mater. 6 (2007) 13.
[2] Y. Tokura, S. Seki, Adv. Mater. 22 (2010) 1554.
[3] H. Katsura, N. Nagaosa, A.V. Balatsky, Phys. Rev. Lett. 95 (2005) 057205.
[4] N. Hur, S. Park, P.A. Sharma, J.S. Ahn, S. Guha, S-W. Cheong, Nature (London) 429 (2004) 392.
[5] J.A. Alonso, M.T. Casais, M.J. Martínez-Lope, J.L. Martínez, M.T. Fernández-Díaz, J. Phys.: Condens. Matter 9 (1997) 8515.
[6] I. Kagomiya, K. Kohn, T. Uchiyama, Ferroelectrics 280 (2002) 131.
[7] P.G. Radaelli, L.C. Chapon, J. Phys.: Condens. Matter. 20 (2008) 434213.
[8] C. Doubrovsky, G. André, A. Goukassov, P. Auban-Senzier, C.R. Pasquier, E. Elkaim, M. Li, M. Greenblatt, F. Damay, P. Foury-Leylekian, Phys. Rev. B 86 (2012) 174417.
[9] G.R. Blake, L.C. Chapon, P.G. Radaelli, S. Park, N. Hur, S.-W. Cheong, J. Rodriguez-Carvajal, Phys. Rev. B 71 (2005) 214402.
[10] J. Koo, C. Song, S. Ji, J.-S. Lee, J. Park, T.-H. Jang, C.-H. Yang, J.-H. Park, Y.H. Jeong, K.-B. Lee, T.Y. Koo, Y.J. Park, J.-Y. Kim, D. Wermeille, A.I. Goldman, G. Srajer, S. Park, S.-W. Cheong, Phys. Rev. Lett. 99 (2007) 197601.
[11] A. Mu noz, J.A. Alonso, M.T. Casais, M.J. Martínez-Lope, J.L. Martínez, M. T. Fernández-Díaz, Eur. J. Inorg. Chem. 2005 (2005) 685.
[12] G. Buisson, Phys. Status Solidi A 17 (1973) 191.
[13] I.A. Zobkalo, S.V. Gavrilov, N.Z. Saw Nyi, S.N. Barilo, S.V. Shiryaev, J. Magn. Magn. Mater. 354 (2014) 85.
[14] C. Doubrovsky, G. Andre, F. Bouquet, E. Elkaim, M. Li, M. Greenblatt, P. Foury-Leylekian, Physica B 407 (2012) 1718.
[15] A.P. Ramirez, Czechoslov. J. Phys. 46 (1996) 3247.
[16] A.B. Sushkov, R.V. Aguilar, S. Park, S-W. Cheong, H.D. Drew, Phys. Rev. Lett. 98 (2007) 027202.
[17] A.B. Sushkov, M. Mostovoy, R.V. Aguilar, S.-W. Cheong, H.D. Drew, J. Phys.: Condens. Matter 20 (2008) 434210.
[18] J. Rodriguez-Carvajal, Physica B 192 (1993) 55.